

# Nonstationary Model of the Semicontinuous Depolymerization of Polycarbonate

Raúl Piñero-Hernanz, Juan García-Serna, and María José Cocero

Dept. of Chemical Engineering and Environmental Technology, University of Valladolid, Valladolid, Spain

DOI 10.1002/aic.11025

Published online October 30, 2006 in Wiley InterScience (www.interscience.wiley.com).

*The experimental work for the depolymerization process of Bisphenol A polycarbonate pellets and CD/DVD wastes in a semicontinuous reactor and a novel nonstationary model to describe the process is presented. The different steps of the process to develop the model are analyzed thoroughly. The kinetics of the alkali-catalyzed methanolysis of polycarbonate was determined. The reactor and kinetic models were validated by a series of 21 experiments performed in a laboratory semicontinuous tubular reactor at isothermal conditions from 90 to 180°C and pressures from 1.0 to 20.0 MPa in liquid phase, with and without NaOH concentrations of  $1 \times 10^{-3}$  to  $5 \times 10^{-3}$  kg/L, flow rates from  $2.3 \times 10^{-3}$  to  $10.2 \times 10^{-3}$  L/min, and CO<sub>2</sub> molar fractions from zero to 0.374. The effects of temperature, pressure, catalyst amount, mass transfer (solvent flow rate), and CO<sub>2</sub> addition in kinetics were investigated. © 2006 American Institute of Chemical Engineers AIChE J, 52: 4186–4199, 2006*

**Keywords:** Bisphenol A polycarbonate, nonstationary model, chemical recycling, depolymerization, kinetics

## Introduction

Bisphenol A-based polycarbonate (BPA-PC) has been used extensively in the manufacture of optical discs (CDs and DVDs) since 1982 when PolyGram launched the first audio-CD. BPA-PC is used in a large variety of plastic materials, mainly in the electronic sector (54%), construction (20%), and automotive sector (10%). Vast amounts of wastes of BPA-PC-made products are currently generated as a consequence of the increasing consumption of these cradle-to-grave products. This situation might cause serious environmental damage in the future because BPA is an extremely toxic compound that can pass to the water streams, which is a major threat to natural ecosystems. Data storage systems have been reengineered considerably with the invention of pen-drive memories without moving parts, getting closer to what Nature does for instance in the brain. Novel optical discs, made of biodegradable polymers, such as the paper-based Blu-ray Disc from Sony and

Toppan Printing follow many of the recommendations of green engineering<sup>1,2</sup> and biomimicry.<sup>3</sup>

In the next years it will be of essential importance to approach sustainability in this sector, getting-to-zero waste<sup>4</sup> by reuse (such as rewritable discs), physical recycling (such as mechanical layer removal; Universal Manufacturing & Logistics, Santa Monica, CA), or chemical recycling recovering the start-up monomers and other side products. By changing the actual cradle-to-grave approach into a cradle-to-cradle approach the industry will be able to solve this imminent problem.<sup>5</sup> Currently, tons of CD/DVD wastes per year are incinerated or buried in dumps. Mechanical or physical recycling requires a special fabrication process that allows for the easy removal of the metal data-storage layer. Apparently, chemical recycling is a more universal alternative, allowing for the recycling of a range of disc formats from different producers, although it is energy and material intensive.

Several BPA-PC depolymerization processes have been reported so far. In 1989 Fox and Peters<sup>6</sup> patented a process using methylene chloride with ammonia as solvent in combination with an alkali catalyst that was successfully applied for PC decomposition. In 1994 Shafer<sup>7</sup> patented a depolymerization process that used phenol as a solvent and also an alkali catalyst. Both processes used highly toxic solvents and implied a compli-

Correspondence concerning this article should be addressed to J. García-Serna at jgserna@iq.uva.es.

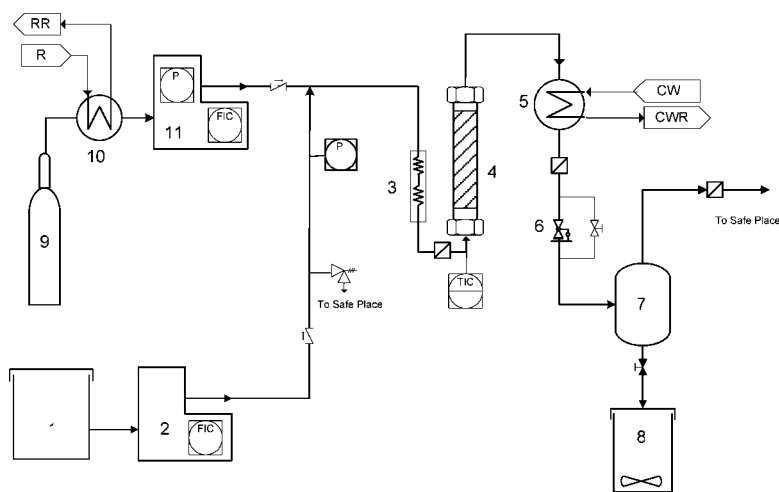


**Figure 1. Flow diagram of the semicontinuous lab plant for polycarbonate recycling.**

(1) Solvent storage tank; (2) high-pressure pump; (3) preheater (integrated within reactor); (4) reactor; (5) product cooler; (6) back-pressure regulator; (7) flash vessel; (8) product storage tank; (9) CO<sub>2</sub> cylinder; (10) CO<sub>2</sub> chiller; (11) CO<sub>2</sub> high-pressure pump.

cated product separation and possible environmental safety problems. Moreover, batch experiments for BPA-PC decomposition carried out by Hu et al.<sup>8</sup> showed that alkali-catalyzed methanolysis can be achieved at low temperatures (40–60°C) and atmospheric pressure, although very low yields (about 7 wt %) of Bisphenol A were obtained. Furthermore, the process required long reaction times (about 330 min) and a mixture of methanol and toluene to decrease the reaction time and increase the BPA yield to 90–96 wt %. Aliphatic alcohols at supercritical conditions deserve special attention as an alternative reaction media because under such conditions mass transfer and kinetics are enhanced. On the other hand, the studies of Yang et al.,<sup>9</sup> Goto et al.,<sup>10</sup> and recently Genta et al.<sup>11</sup> focused on the recycling of poly(ethylene terephthalate) (PET) by methanolysis under supercritical or near-critical conditions, obtaining excellent results with fast kinetics and a high degree of selective depolymerization. Our research group<sup>12</sup> conducted a preliminary feasibility study on the depolymerization of PC using an alkali-catalyzed methanolysis at near-critical conditions.

Sterling and McCoy<sup>13</sup> studied the different reaction pathways of degradation and depolymerization of polymers based in stochastic models. In their study the authors briefly reviewed the main models used for depolymerization. Wan et al.<sup>14</sup> modeled the depolymerization of PET in a potassium hydroxide solution using a stirred-batch reactor to determine the initial rates of reaction. Results are in good agreement with experimental data only at low conversions. Park et al.<sup>15</sup> studied the depolymerization of styrene–butadiene copolymer in near-critical and supercritical water in a batch reactor using a detailed statistical analysis. Kao et al.<sup>16</sup> determined the kinetics of hydrolytic depolymerization of melting PET in a batch reactor considering an autocatalytic mechanism. McCoy and Wang<sup>17</sup> used a continuous flow stirred tank reactor (CSTR) equation.

This article presents a novel nonstationary modeling of the process of depolymerization of Bisphenol A polycarbonate considering a shrinking particle model with surface end-chain reaction for the pellets and a series of  $n$  tanks for the semicontinuous reactor. This model is used to determine kinetic parameters of the alkali-catalyzed methanolysis of BPA-PC.

Raw polymer pellets and crushed CD/DVD wastes were depolymerized producing equimolar quantities of BPA and dimethyl carbonate (DMC). DMC is an excellent solvent that can be reused for the cleaner production of BPA-PC without using phosgene.<sup>18</sup> The reaction was investigated in a  $20 \times 10^{-3}$  L laboratory reactor at isothermal conditions from 90 to 180°C and pressures from 1.0 to 20.0 MPa in liquid phase, operating under semicontinuous mode. A model of the reaction process is presented considering a shrinking particle model for the pellets and a series of  $n$  perfectly mixed tanks for the reactor. The extents and kinetics of the reaction of polycarbonate particles as a function of temperature, pressure, catalyst amount, and flow rate were determined using on-line high-performance liquid chromatography (HPLC) and gas chromatography (GC) sample analysis. The effect of CO<sub>2</sub> addition was also investigated.

## Experimental

### Chemicals and materials

Polycarbonate (PC) pellets with a particle size of  $3 \times 10^{-3}$  m length  $\times$   $2 \times 10^{-3}$  m diameter were supplied by GEPESA (GE Plastics Iberica S.A., Barcelona, Spain). Methanol (analytical grade) and sodium hydroxide (>99 % purity) were purchased from Aldrich and used without further modification. Wastes coming from CD/DVD residues were collected for the PC recycling tests. CD/DVD wastes were previously crushed into pieces ( $5 \times 10^{-3}$ – $5 \times 10^{-3}$  m size), then washed with hot deionized water (70°C), and finally dried at 103°C before being charged into the reactor.

### Experimental equipment: semicontinuous lab plant

A flow diagram of the reaction system is shown in Figure 1. The lab plant was designed to operate under a wide range of operating conditions: temperatures from 20 to 400°C, pressures from 0.1 to 30 MPa, and flow rates from  $0.1 \times 10^{-3}$  to  $20 \times 10^{-3}$  L/min of organic and  $0.1 \times 10^{-3}$  to  $15 \times 10^{-3}$  L/min of

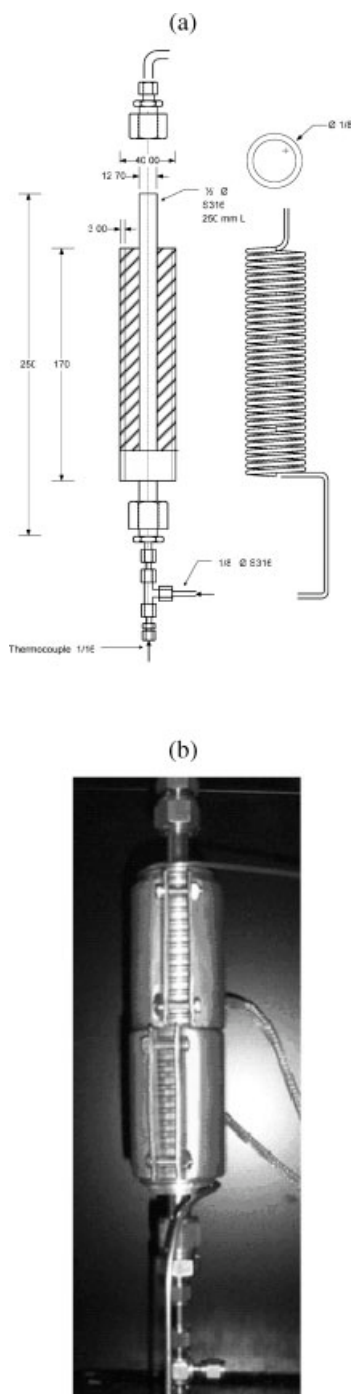


**Figure 2. Reactor mechanical design and overview.**

(a) Reactor mechanical design; (b) overview photograph showing how the preheater is a coil rolled over an aluminum block in which the reactor is enclosed.

CO<sub>2</sub>. BPA-PC pellets are charged into the tubular reactor (internal volume  $\cong 20 \times 10^{-3}$  L). The experimental apparatus is provided with an easy-opening tubular reactor developed to perform experiments in semicontinuous mode. The special design of the reactor aims to optimize the heat transfer and minimize the size of the plant by integrating the preheater and

the reaction zone in one module (Figure 2). A methanol–NaOH solution is pumped and preheated before entering the reactor where reaction with the polycarbonate takes place. The reactor is equipped with an aluminum heating block provided with band heaters and K-type thermocouples connected to a PID controller set at the desired temperature value. A manual back-pressure regulator valve controls the pressure of the system, depressurizing the outlet stream to atmospheric conditions before entering a flash vessel. From this flash vessel the products of the reaction flow to the final collecting stirred vessel by gravity flow.

During the experiment liquid samples are collected from both the flash vessel (instant concentration) and from the collecting stirred flask (accumulated concentration). The samples were subsequently analyzed by HPLC and GC.

### Analytical techniques

The initial raw material was characterized using DSC (differential scanning calorimetry) to check the rheological and phase-transition behavior of both commercial PC pellets and CD wastes. Analyses were performed on a DSC 822e (Mettler-Toledo SAE, Barcelona, Spain), equipped with an FSR 5 ceramic detector (temperature range 153–973 K, resolution  $< 0.04 \mu\text{W}$ , sensibility  $15 \mu\text{V}$ ). PC samples were prepared in disk shape (10 mg); DSC measurements were run by heating from 303 to 523 K at 20 K/min with inert atmosphere (N<sub>2</sub>,  $60 \times 10^{-3}$  L/min).

Analyses of the reaction products were carried out using HPLC and GC to quantify Bisphenol A and DMC, respectively. HPLC analyses were performed on a Waters separation module equipped with a UV detector (Waters 2487 Dual  $\lambda$  Absorbance, Waters, Milford, MA) set at 254 nm and using a Waters C-18 LC column (5  $\mu\text{m}$  particle size,  $4.6 \times 10^{-3} \times 250 \times 10^{-3}$  m). An isocratic method was used: acetonitrile and buffer solution (acetic acid/sodium acetate) were used as mobile phase (45:55 v/v) and pumped at a constant flow rate ( $1 \times 10^{-3}$  L/min, 40°C). The reaction samples were diluted 1:25 with methanol. DMC and the remaining volatile products were analyzed by GC. Liquid samples were analyzed on HP 5890 GC equipment (Agilent Technologies, Santa Clara, CA) with a TCD using helium as carrier fluid. The products were separated by a HayeSep P column (3 m  $\times$  1/8-in., 60–80  $\mu\text{m}$ ; Teknokroma, Barcelona, Spain). The temperatures of the detector and the injector port were 200 and 150°C, respectively; the method was set up to follow a gradient of temperature from 80 to 180°C. The samples (3  $\mu\text{L}$  of volume injection) were diluted 1:5 in methanol.

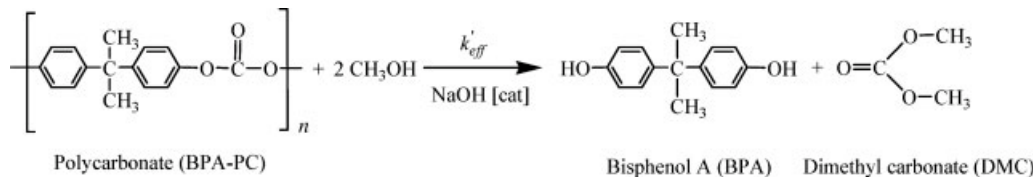
Separation and purification of Bisphenol A were achieved by crystallization in water with further filtration and drying at 104°C to eliminate the residual water and volatile compounds. The final crystallized product was filtrated, dried, and chemically characterized by Fourier transform infrared (FTIR) spectroscopy. IR spectra were generated using a Bruker tensor FTIR spectrometer model (Bruker Española, Madrid, Spain) equipped with a DLATGS (deuterated L- $\alpha$  alanine doped with tryglycine sulfate) detector, and a Golden Gate ATR (attenuated total reflectance) accessory. Analyses were performed with a spectra resolution of  $4 \times 10^{-2} \text{ m}^{-1}$  and measured eight scan times. Absorbance spectra were measured in the wave-number infrared region 40–6  $\text{m}^{-1}$ .

## Mechanism of Reaction

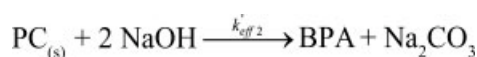
In the degradation of BPA-PC in methanol at high temperatures and pressures, the two extreme reaction paths studied by Sterling and McCoy<sup>13</sup> and Madras and McCoy<sup>19,20</sup> may represent the reactions to produce monomeric species from the polymer. The first alternative considers pure random degradation, represented by binary scission of bonds at any position along the chain as adopted by Goto et al.<sup>21</sup> for the degradation of PET in supercritical methanol. Recently, Iwaya et al.<sup>22</sup>

from the same research group considered the other extreme specific reaction, which releases monomeric species of the polymer by scission at the chain end, for the hydrothermal decomposition of Nylon 6.

Our research group studied the alkali-catalyzed degradation of BPA-PC in near-critical methanol to recover BPA and DMC. Based on our experimental results, described later, the major reaction for the monomerization of BPA-PC in methanol and the side reactions considered were:



Scheme 1



Scheme 2



Scheme 3

Decomposition of polycarbonate in the presence of methanol and an alkali catalyst can be described by different mechanisms of reaction that imply basically two possibilities: (1) alkali-catalyzed methanolysis and (2) alkali reaction in solution without methanol consumption. In Scheme 1, methanol acts both as solvent and reagent, whereas the alkali (NaOH) increases the reaction rate only as catalyst. Scheme 2 implies the consumption of NaOH as reagent with no reaction of methanol, which acts only as a solvent. The presence of Na<sub>2</sub>CO<sub>3</sub> was detected qualitatively, however, no quantitative analysis was conducted for this compound and thus  $k'_{\text{eff}2}$  was not included in the fit. Scheme 3 considers the side production of phenol by BPA decomposition. The unknown compound (“Other”) indicates that several different minority components may be formed.

## Theoretical Model

### Model assumptions

To model the reactive-dissolution of the BPA-PC particles the nonstationary approach assuming a shrinking particle model proposed by Schmidt<sup>23</sup> was considered. A schematic approach to the physical system is presented in Figures 3 and 4a and 4b. The primary assumptions of the physical approach are as follows:

(1) The polymer is homogeneously distributed inside each particle so that the concentration of BPA-PC is constant within the particle. The particles are nonporous so the reaction takes place in the surface of the particles. The size of the particles decreases along with reaction time.

(2) The reagent, which flows up-flow round the particle, is first transferred into the stagnant fluid layer surrounding the

particle and afterward it reacts on the surface of the particle with pure BPA-PC (see Figure 3).

(3) As a result of this two-step process, that is, mass transfer and reaction, and considering first-order kinetics, the rate of reaction constants calculated will refer to the effective rate of reaction,  $1/k_{\text{eff}} = 1/k_f + 1/k_{sr}$ .

(4) Density and viscosity are considered constant along the reactor and are similar to values of the solvent properties. This assumption is valid at lab-scale conditions. The addition of a thermodynamic model [equation of state (EoS)] considering the multicomponent mixture to the set of equations is strongly recommended to predict fluid-phase equilibria and physical properties if the scale-up of the system is required.

(5) Monomeric species of the polymer are formed by scission at the chain end in all cases.

The real reaction process will be a mixture of the two cases illustrated in Figures 4a and 4b. At the beginning, when the particles are too large and remain static, the reactor can be considered a fixed bed. During the reaction the particles shrink and at some point the particles are fluidized and the reactor can be considered to be perfectly mixed. The modeling of the fixed-bed reactor enormously complicates the simulation because as the particle diameter decreases, layers move down and the equation needs to consider the moving boundary of each layer. Moreover, random relocations of the particles within the layers and even exchange of particles between layers should be considered, which adds extra simulation time. To simplify the model's mathematical solution, it has been considered that the particles behave like a perfectly mixed vessel because the reactor is small and because of the backmixing created by the turbulences (eddies) generated in the fluid around the particles. Considering all this, the primary assumptions of the model are as follows:

- (1) The number of particles is constant during the experiment until the reaction is completed.
- (2) A series of perfectly mixed reactors are used to simulate the layer effect. The number of particles in each layer is predetermined and constant. Axial and radial concentration and temperature gradients are negligible.
- (3) To obtain the maximum information of the system, the product vessel has been included within the model equations considering the nonstationary accumulation of the different compounds.

### Mass balance for the polymer pellets

The material balance for the solid polycarbonate phase (component 1) considers homogeneous reaction in the surface of the pellets in a hypothetically perfectly mixed vessel:

$$\frac{dm_k}{dt} = [MW_1(\alpha_{11}F_1 + \alpha_{21}F_2)]_k \quad (1)$$

### Mass balance for the fluid components

The matrix of the eight components is: {PC MeOH BPA DMC NaOH Na<sub>2</sub>CO<sub>3</sub> PhOH Other}.

The molar balance to the component  $j$  in the liquid phase for a perfectly mix tank reactor  $k$  is given by

$$\frac{d(n_j)_k}{dt} = \dot{v}[(c_j)_{k-1} - (c_j)_k] \quad j = 2 \dots 8 \quad (2)$$

$$\frac{d(n_j)_k}{dt} = \frac{d(V_{\text{reactor}}c_j\varepsilon)_k}{dt} = \left[ V_{\text{reactor}} \left( \varepsilon \frac{dc_j}{dt} + c_j \frac{d\varepsilon}{dt} \right) \right]_k \quad j = 2 \dots 8 \quad (3)$$

$$\frac{d(c_j)_k}{dt} = \frac{1}{\varepsilon_k} \left\{ \frac{\dot{v}}{(V_{\text{reactor}})_k} [(c_j)_{k-1} - (c_j)_k] + \frac{\alpha_j F_k}{(V_{\text{reactor}})_k} + (c_j)_k \left[ \frac{\alpha_1 F_k MW_1}{\rho_{\text{PC}}(V_{\text{reactor}})_k} \right] \right\} \quad j = 2 \dots 8 \quad (4)$$

### Bed void volume fraction (BVVF) change

BVVF of the bed is defined as the ratio of void volume (filled with liquid) and the total volume of the reactor. BVVF increases along with reaction as a result of the consumption of PC during the reaction as follows:

$$\frac{d\varepsilon_k}{dt} = -\frac{\alpha_1 F_k MW_1}{\rho_{\text{PC}}(V_{\text{reactor}})_k} \quad (5)$$

In addition to this, the instant BVVF can also be estimated directly from the unreacted mass of polymer and the total volume of the reactor as follows:

$$\varepsilon_k = 1 - \frac{m_k}{\rho_{\text{PC}}(V_{\text{reactor}})_k} \quad (6)$$

### Material accumulation in the product vessel

The nonstationary material balance at the outlet of the  $n$ th tank matches values at the entrance of the final product vessel, which is a graduated flask:

$$\frac{dV^{\text{flask}}}{dt} = \dot{v} \quad (7)$$

$$V^{\text{flask}} \frac{dc_j^{\text{flask}}}{dt} + c_j^{\text{flask}}(\dot{v}) = \dot{v}(c_j - 0) \quad (8)$$

$$\frac{dc_j^{\text{flask}}}{dt} = \frac{\dot{v}}{V^{\text{flask}}} (c_j - c_j^{\text{flask}}) \quad j = 2 \dots 8 \quad (9)$$

$$\frac{dm_j^{\text{flask}}}{dt} = \dot{v} c_j MW_j \quad j = 2 \dots 8 \quad (10)$$

### Other physicochemical parameters

The volume of reactor is computed as the volume of the bare tube:

$$(V_{\text{reactor}})_k = \frac{1}{n} 1000 \pi R^2 L_{\text{reactor}} \quad (11)$$

The generation function  $F$  is a three-component vector that depends on the kinetic rate coefficients, reagent concentrations, and surface area of the pellets (Eq. 12). The surface is estimated considering that the initial number of particles is constant and is composed of spherical-like particles (Eq. 13).

$$F_k = [k'_{\text{eff}1}(c_2)_k a_k \quad k'_{\text{eff}2}(c_5)_k a_k \quad k_3(c_3)_k (V_{\text{reactor}})_k \varepsilon_k] \quad (12)$$

$$a_k = (n_p a_p)_k = n_p 4\pi \left( \frac{3}{n_p 4\pi \rho_{\text{PC}}} \right)^{2/3} m_k^{2/3} \quad (13)$$

The matrix of stoichiometric coefficients and molecular weights of reactions are, respectively,

$$\alpha = \begin{bmatrix} -1 & -2 & 1 & 1 & 0 & 0 & 0 & 0 \\ -1 & 0 & 1 & 0 & -2 & 1 & 0 & 0 \\ 0 & 0 & -1 & 0 & 0 & 0 & 1 & 1 \end{bmatrix} \quad (14)$$

$MW$

$$= [0.254 \quad 0.0320 \quad 0.228 \quad 0.0901 \quad 0.040 \quad 0.106 \quad 0.094 \quad 0.134] \quad (15)$$

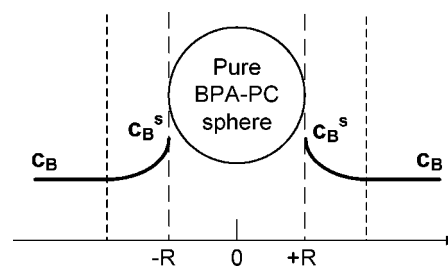
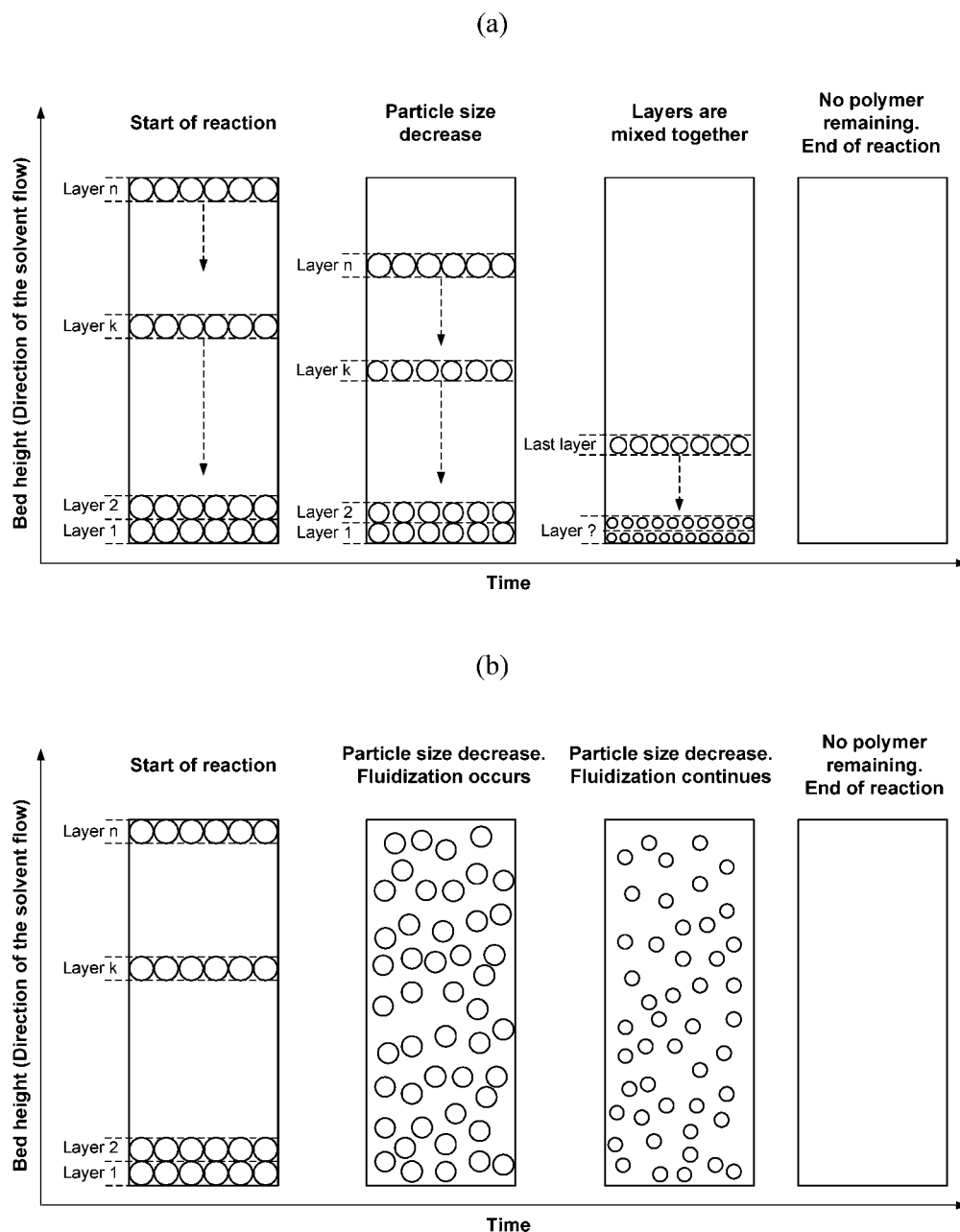


Figure 3. Concentration profiles during reactive dissolution.



**Figure 4. Evolution of the polymer pellets in the reactor.**

(a) Stable fixed bed of pellets; (b) fluidized bed of pellets.

### Numerical solution strategy

A final set of nine ordinary differential equations (ODEs) formed by Eqs. 1, 4, and 5, with respect to a perfectly mixed reactor, plus 15 ODEs from Eqs. 7, 9, and 10 was solved using a modified second-order Rosenbrock formula<sup>24</sup> using MATLAB<sup>®</sup> 7.0 R14 (The MathWorks, Natick, MA).

Therefore, the simplified model has four adjustable parameters: the kinetic rates ( $k_{eff1}$ ,  $k_{eff2}$ , and  $k_3$ ) and the number of tanks  $n$ , estimated by minimizing the errors between experimental and calculated yield values of Bisphenol A and sodium carbonate and phenol using a Simplex method. The errors were quantified by defining average absolute deviation (%AAD) as shown in Eq. 16, where  $n_{data}$  represents the num-

ber of data and  $y_{experimental}$  and  $y_{calculated}$  are the data obtained from experiments and model equations, respectively, at the  $l$ th condition.

$$AAD (\%) = \frac{1}{n_{data}} \sum_{l=1}^{n_{data}} \left| \frac{y_{experimental} - y_{calculated}}{y_{experimental}} \right| \times 100 \quad (16)$$

The measured density of polycarbonate particles ( $\rho_{PC}$ ) was 1100 kg/m<sup>3</sup> and the calculated BVVF at initial conditions was between 0.73 and 0.84 m<sup>3</sup>/m<sup>3</sup>. The density of methanol at reaction conditions was estimated using Aspen Plus<sup>®</sup> 12.1 (Aspen Technology, Cambridge, MA) with the NRTL EoS.



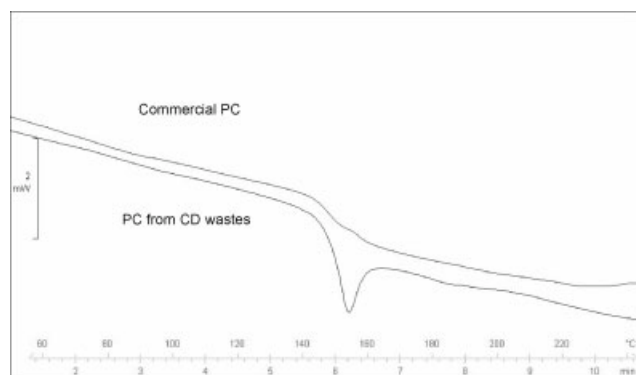


**Figure 5. DSC analysis of commercial polycarbonate (PC) and PC from CD wastes.**

Glass-transition temperature located at 149.24 and 147.25°C, respectively.

## Results and Discussion

### Characterization of the raw material: DSC analysis

Polycarbonate is an amorphous polymer with a distinct glass transition around 150°C. The glass-transition point indicates the temperature at which the polymer undergoes a change of phase where it loses its rigid solid form and starts to flow. Around this point, the mass-transport properties of the polymer (especially diffusivity) are much more favorable to cause degradation of the plastic by means of a fluid–fluid reaction. Both commercial PC pellets and CD/DVD wastes were characterized by DSC to determine their glass-transition points and to compare their thermodynamic and rheological behaviors. The resulting DSC curves are given in Figure 5 and show similar behavior for both materials. These two materials exhibit a glass-transition temperature ( $T_{gt}$ )

slightly <150°C (149.24 and 147.25°C, for the commercial PC and CD/DVD wastes, respectively). The phase change is an endothermic process and the melting enthalpy cannot be determined because both materials are amorphous. Regarding the CD/DVD material, the DSC curve is slightly sharper at the transition point resulting from the different thermal history of the polymer, but, in general, they are quite similar materials.

### Purity analysis of the BPA produced

FTIR spectroscopy analyses of the commercial pure Bisphenol A and the crystallized final product obtained from CD/DVD wastes were conducted. The overlaid spectra are nearly identical, which confirms the acceptable purity of the final product as illustrated in Figure 6.

### Design of experiments

A design of experiments (DoE) was prepared to investigate the influence of the operational parameters: temperature, pressure, and NaOH concentration and, subsequently, to carry out a statistical analysis of the results to verify the reproducibility of the experimental data and to give a rough estimation of the variables' importance on the yield and reaction rate of the process. From the several possibilities used to prepare the DoE table, the orthogonal arrangement with a set of nine experiments (entries 1 to 9) as shown in Table 1 was chosen. Eight additional experiments were conducted to study the influence of temperature in entries 10 to 13 (Arrhenius parameters) and mass transfer in entries 14 to 17 (flow rate). Finally, runs 18 to 21 studied the influence of CO<sub>2</sub> addition to the solvent flow rate at the reactor inlet. The results, including product yields and operational time, are listed in Table 1.

BPA, DMC, and PhOH yields were calculated as the ratio of the produced amount and the maximum theoretical production

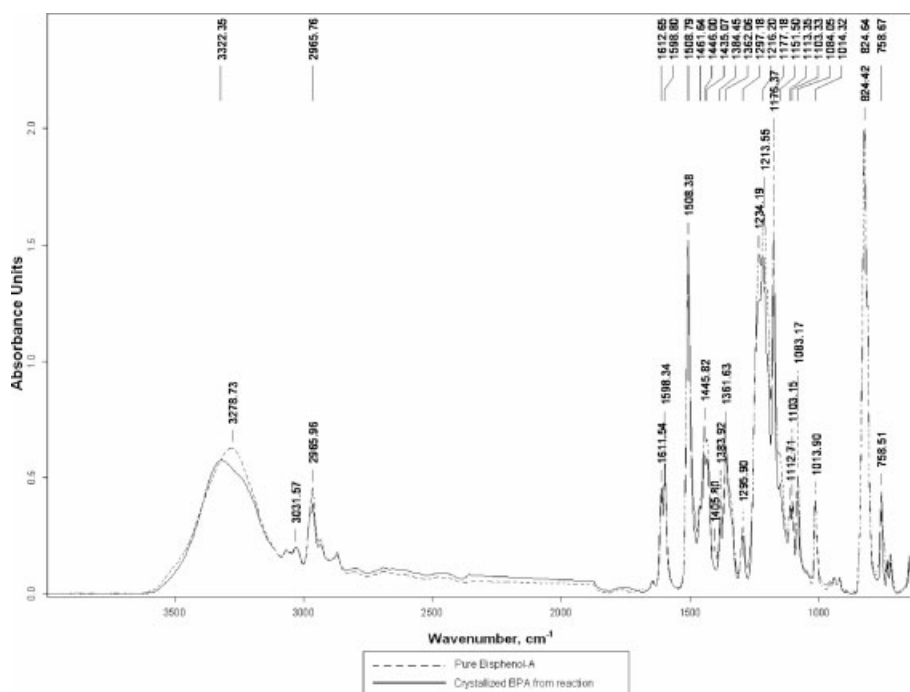


**Figure 6. FTIR analysis for purity check.**

Table 1. Design of Experiments: Summary of Results

Run	T (°C)	P (MPa)	[NaOH] (kg L <sup>-1</sup> )	MeOH Flow (L/min)	CO <sub>2</sub> (% mol)	Initial Mass* (kg)	OT** (min)	BPA Yield (wt %)	PC Conv. (%)	DMC Yield (wt %)	PhOH Yield (wt %)	$k_{eff}$ (min <sup>-1</sup> L <sup>-1</sup> m <sup>-2</sup> )	$k_3$ (min <sup>-1</sup> )
1	105	20.0	2.0 × 10 <sup>-3</sup>	2.26 × 10 <sup>-3</sup>	0	10.012 × 10 <sup>-3</sup>	70	97.4	100	90.9	1.7	—	—
2	150	20.0	2.0 × 10 <sup>-3</sup>	2.23 × 10 <sup>-3</sup>	0	9.997 × 10 <sup>-3</sup>	63	95.4	100	80.3	1.8	—	—
3	180	20.0	2.0 × 10 <sup>-3</sup>	2.33 × 10 <sup>-3</sup>	0	10.005 × 10 <sup>-3</sup>	—	92.6	100	—	2.8	—	—
4	180	20.0	2.0 × 10 <sup>-3</sup>	2.88 × 10 <sup>-3</sup>	0	9.990 × 10 <sup>-3</sup>	52	95.4	100	77.5	1.8	—	—
5	150	1.0	2.0 × 10 <sup>-3</sup>	2.32 × 10 <sup>-3</sup>	0	10.023 × 10 <sup>-3</sup>	64	85.9	100	71.3	3.0	—	—
6	180	10.0	2.0 × 10 <sup>-3</sup>	2.47 × 10 <sup>-3</sup>	0	10.001 × 10 <sup>-3</sup>	64	92.5	100	82.4	1.9	—	—
7	140	20.0	0.0	2.27 × 10 <sup>-3</sup>	0	10.008 × 10 <sup>-3</sup>	108	81.7	80.0	75.3	2.3	—	—
8	140	20.0	5.0 × 10 <sup>-3</sup>	2.25 × 10 <sup>-3</sup>	0	9.990 × 10 <sup>-3</sup>	60	92.2	100	76.3	1.4	—	—
9	140	20.0	1.0 × 10 <sup>-3</sup>	2.09 × 10 <sup>-3</sup>	0	9.979 × 10 <sup>-3</sup>	70	92.3	100	75.9	1.5	—	—
10	90	10.0	2.0 × 10 <sup>-3</sup>	10.2 × 10 <sup>-3</sup>	0	6.880 × 10 <sup>-3</sup>	62	97.8	100	83.6	0.2	0.30	0.0023
11	105	10.0	2.0 × 10 <sup>-3</sup>	7.65 × 10 <sup>-3</sup>	0	6.886 × 10 <sup>-3</sup>	34	98.3	100	91.4	0.3	0.76	0.0034
12	120	10.0	2.0 × 10 <sup>-3</sup>	7.6 × 10 <sup>-3</sup>	0	7.905 × 10 <sup>-3</sup>	22	98.4	100	87.4	0.4	3.20	0.0061
13	140	10.0	2.0 × 10 <sup>-3</sup>	8.33 × 10 <sup>-3</sup>	0	6.884 × 10 <sup>-3</sup>	21	98.0	100	84.8	0.4	8.50	0.0087
14	120	10.0	2.0 × 10 <sup>-3</sup>	2.28 × 10 <sup>-3</sup>	0	6.207 × 10 <sup>-3</sup>	56	91.0	100	82.0	1.3	0.60	0.0015
15	120	10.0	2.0 × 10 <sup>-3</sup>	3.08 × 10 <sup>-3</sup>	0	7.997 × 10 <sup>-3</sup>	38	97.4	100	81.9	0.5	0.76	0.0023
16	120	10.0	2.0 × 10 <sup>-3</sup>	7.6 × 10 <sup>-3</sup>	0	7.901 × 10 <sup>-3</sup>	21	98.4	100	91.0	0.5	3.20	0.0065
17	120	10.0	2.0 × 10 <sup>-3</sup>	10.22 × 10 <sup>-3</sup>	0	6.785 × 10 <sup>-3</sup>	18	96.1	100	94.0	0.5	3.40	0.0090
18	150	20.0	2.0 × 10 <sup>-3</sup>	5.35 × 10 <sup>-3</sup>	9.0	10.010 × 10 <sup>-3</sup>	56	88.6	100	86.0	2.3	—	—
19	150	20.0	2.0 × 10 <sup>-3</sup>	3.67 × 10 <sup>-3</sup>	18.3	9.993 × 10 <sup>-3</sup>	68	85.6	100	70.9	3.2	—	—
20	150	20.0	2.0 × 10 <sup>-3</sup>	2.74 × 10 <sup>-3</sup>	27.7	10.025 × 10 <sup>-3</sup>	N/A	53.7	100	70.1	2.3	—	—
21	150	20.0	2.0 × 10 <sup>-3</sup>	2.18 × 10 <sup>-3</sup>	37.4	9.997 × 10 <sup>-3</sup>	N/A	14.8	100	55.9	0.5	—	—

\* Runs 1–9 and 18–21 correspond to pure polycarbonate Lexan pellets; Runs 10–17 correspond to CD/DVD wastes depolymerization.

\*\* Operational time: indicates the time required to reach 80 wt % of BPA yield during the operation. Nonstationary start-up period is also included in the operation time to include flow effects.



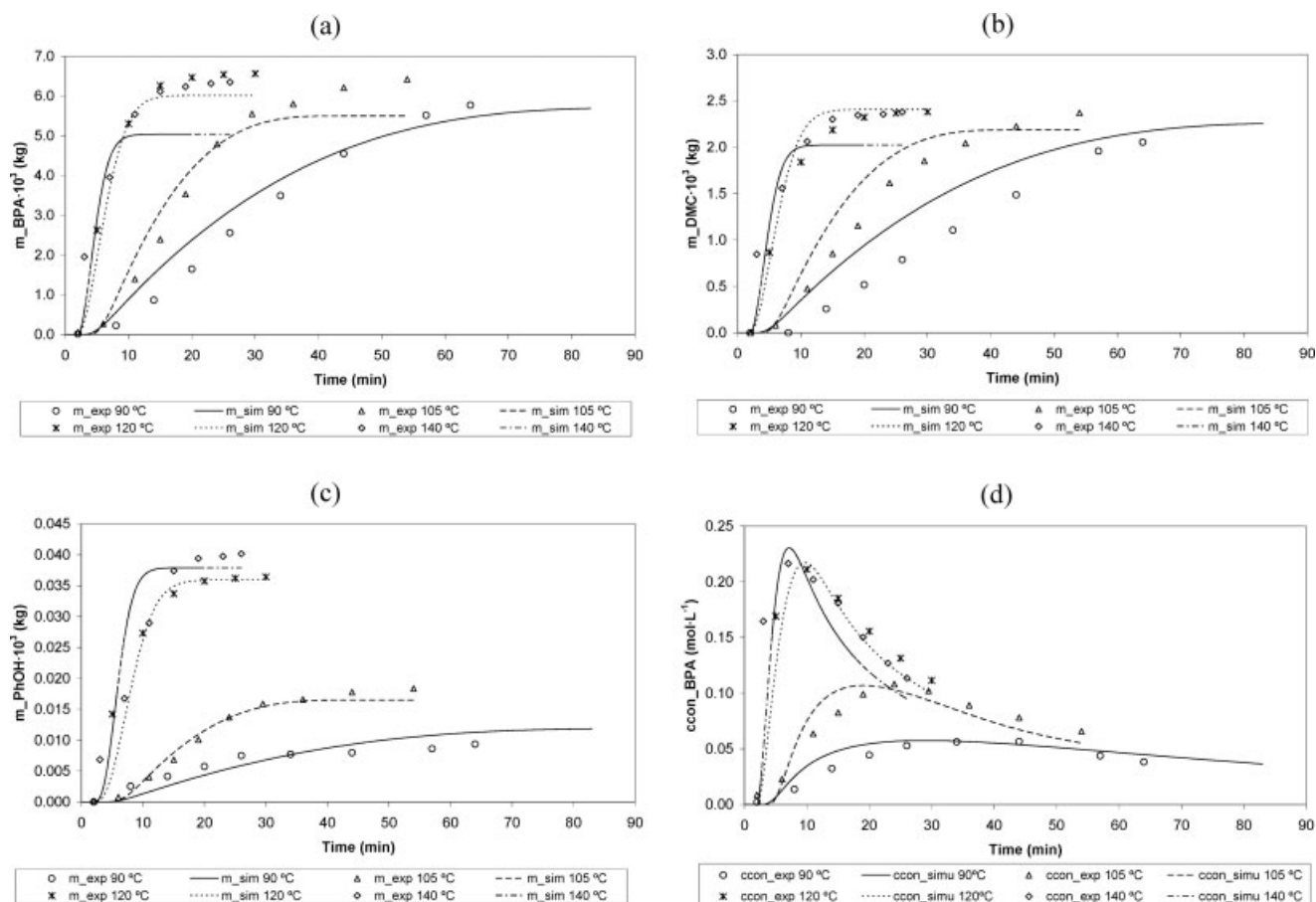


**Figure 7. Experimental and simulated cumulative products at different reaction temperatures.**

(a) Mass of Bisphenol A (BPA); (b) mass of dimethyl carbonate (DMC); (c) mass of PhOH; (d) concentration of BPA in product flask vessel. Pressure = 10 MPa, NaOH =  $2 \times 10^{-3}$  kg/L, flow rate =  $7.7 \times 10^{-3}$ – $10.2 \times 10^{-3}$  L min $^{-1}$ .

from the stoichiometric values (see Eq. 17). For this case, the maximum grams of BPA, DMC, and PhOH per gram of BPA-PC considered were: 89.7 kg BPA/kg BPA-PC, 35.5 kg DMC/kg BPA-PC, and 74.0 kg PhOH/kg BPA-PC, respectively:

$$\text{BPA yield (wt \%)} = \frac{(\text{kg BPA/kg BPA-PC})_{\text{exp}}}{(\text{kg BPA/kg BPA-PC})_{\text{max}}} \times 100 \quad (17)$$

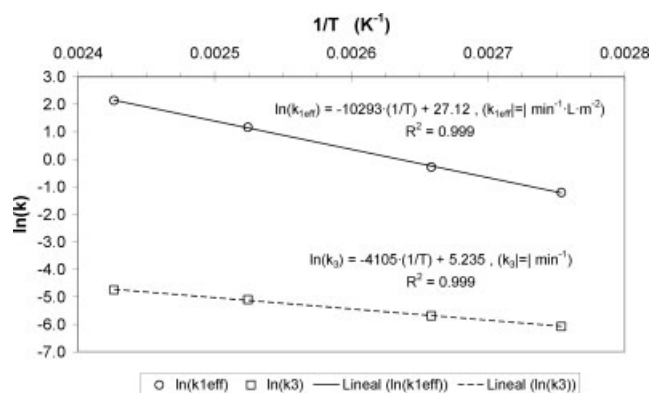
Experiments carried out without alkali catalyst required longer operation times to consume the total initial amount of polymer and were also less selective in terms of BPA and DMC production. Moreover, temperature and pressure seem to be less significant with respect to the BPA and DMC production. BPA yield was between 80 and 98 wt % and DMC was between 65 and 77 wt %. Nevertheless, the experiments conducted at lower pressures and relatively higher temperatures (such as experiment 7) exhibit a significantly lower DMC yield, which may have arisen from the presence of vapor phase in the reaction media or even from a lower residence time in the cooler, which may lead to a partial condensation and thus to a mass loss during the flash separation. On the other hand, the operational time (calculated, in this case, as the required time to obtain 80 wt % of BPA yield) is significantly enhanced by the reaction temperature. These results contrast with the low

yields (7 wt % BPA) obtained when the reaction was carried out in a batch reactor at low temperatures (40–60 °C) with long reaction times (330 min), as reported in the literature.<sup>8</sup>

A partial least-squares (PLS) statistical model, using the DoE table, was developed using SIMCA-P 10.0 software (Umetrics, Umeå, Sweden). The fitting accuracy and predictability of the model according to the experimental data (entries 1 to 9) were evaluated by means of two usual parameters:  $R^2$  (which represents the fraction of variation of the response explained by the model) and  $Q^2$  (which represents the percentage of variation of the response predicted by the model). Unfortunately, for this case the values obtained for these two parameters were  $R^2 = 0.65$  and  $Q^2 = 0.25$ , which means that, even though the fitting of the data is acceptable, the ability of the statistical model to predict new results is limited. Furthermore, the effect of the process parameters was not sufficiently clear using a statistical model for the first nine runs and additional 12 experiments were conducted to understand the effect of the process parameters and validate the proposed model (entries 13 to 21 in Table 1).

#### Effect of reaction temperature

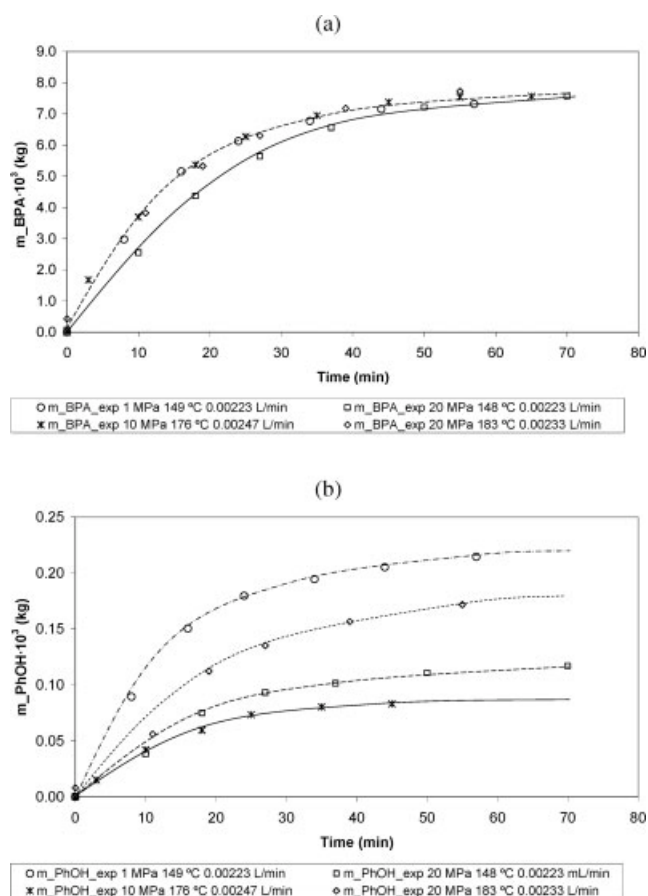
Experiments 10 to 13 were performed at a similar flow rate between  $7.6 \times 10^{-3}$  and  $10.2 \times 10^{-3}$  L min $^{-1}$  using  $2 \times$



**Figure 8. Determination of Arrhenius parameters of the reaction for NaOH =  $2 \times 10^{-3}$  kg L $^{-1}$ .**

Pressure = 10.0 MPa, NaOH =  $2 \times 10^{-3}$  kg/L, flow rate =  $7.7 \times 10^{-3}$ – $10.2 \times 10^{-3}$  L min $^{-1}$ .

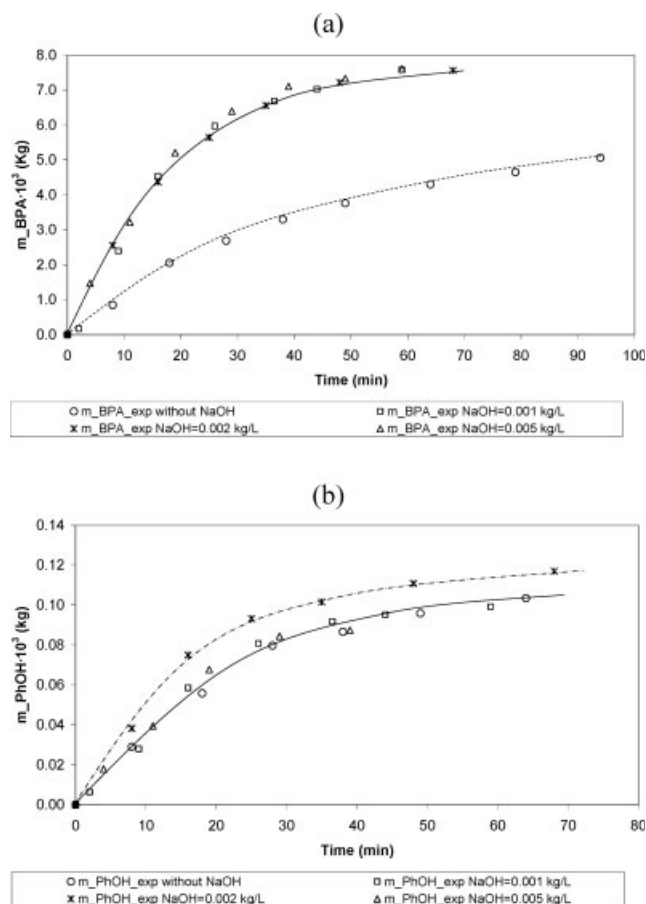
$10^{-3}$  kg L $^{-1}$  of NaOH. Figures 7a–7c illustrate experimental and simulation results of the cumulative mass of products obtained vs. time. It can be seen that almost equimolar production of BPA and DMC was obtained as expressed in the proposed reaction path and that the production increases along with increasing temperatures up to 140°C. Predictions of the



**Figure 9. Experimental cumulative mass of BPA and PhOH products at different pressures.**

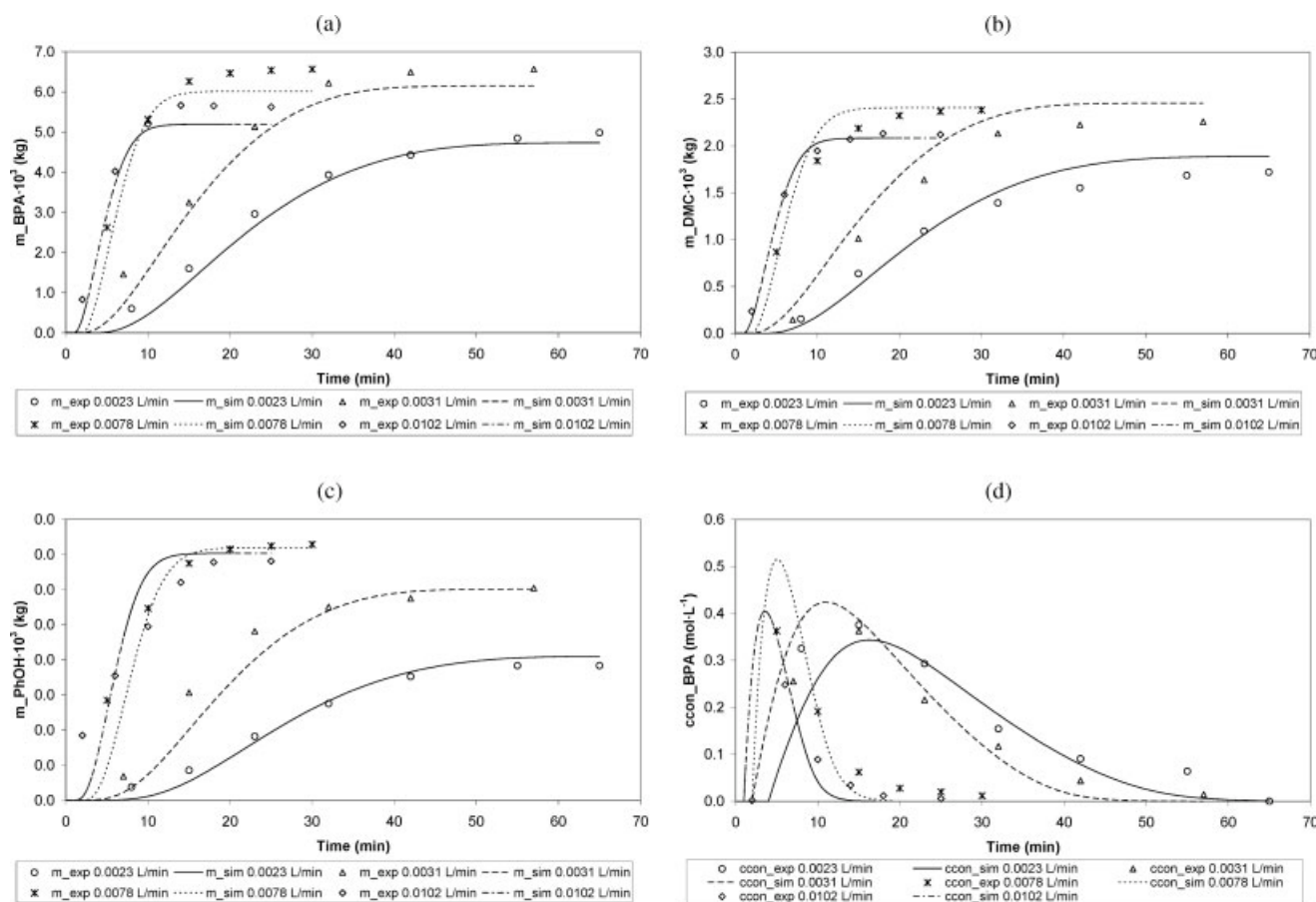
proposed model are in good agreement with experimental data, as shown in Figures 7a–7c and also in Figure 7d, which represents the cumulative concentration of BPA in the product flask vessel with time. Average absolute deviation (ADD%) was between 5 and 15% for all the entries. It must be noted that temperatures  $> 140^\circ\text{C}$  are very close to the glass-transition temperature of the BPA-PC and may cause melting of the polymer inside the reactor. Indeed, temperatures  $\cong 180^\circ\text{C}$  were tested and caused plugging problems in the cooler because of solidification of eventual unreacted melted polymer.

Figure 8 shows the Arrhenius plot of the  $k_{\text{eff}}$  and  $k_3$  values obtained in the range of 363–412 K ( $90$ – $140^\circ\text{C}$ ). The activation energy ( $E_a$ ) was calculated from the slope and the Arrhenius constant ( $A$ ) was calculated from the intercept. Methanolysis activation energy of BPA-PC with respect to BPA production was found to be  $E_{a1} = 87.58$  kJ mol $^{-1}$  and the reaction rate as a function of temperature was:  $k_{\text{eff}} = 6.007 \times 10^{11} \exp(-10,293/T)$  min $^{-1}$  L $^{-1}$  m $^{-2}$  ( $T$  = temperature in Kelvin). Methanolysis activation energy with respect to phenol production was found to be  $E_{a3} = 34.13$  kJ mol $^{-1}$  and the reaction rate as a function of temperature was  $k_3 = 1.876 \times 10^2 \exp(-4105/T)$  min $^{-1}$  ( $T$  = temperature in Kelvin).



**Figure 10. Experimental cumulative mass of BPA and PhOH at different NaOH concentrations at 20 MPa and  $140^\circ\text{C}$ .**

Pressure = 20.0 MPa,  $T = 140^\circ\text{C}$ , flow rate =  $2.1 \times 10^{-3}$ – $2.3 \times 10^{-3}$  L min $^{-1}$ .



**Figure 11. Experimental and simulated cumulative products at different flow rate concentrations.**

(a) Mass of BPA; (b) mass of DMC; (c) mass of PhOH; (d) concentration of BPA at the outlet of reactor. Pressure = 10.0 MPa, NaOH =  $2 \times 10^{-3}$  kg/L,  $T = 120^\circ\text{C}$ .

### Effect of reaction pressure

The reaction has to be performed in the liquid phase, and thus NaOH is used. Thus, pressure must be set at values high enough to ensure monophasic liquid conditions. From the experimental values of BPA production, it seems that the main reaction (Scheme 1) is not influenced by pressure (leading to almost negligible activation volumes), as illustrated in Figure 9a. Nonetheless, Figure 9b shows that the production of phenol is strongly influenced by both pressure and temperature. Thus, phenol production is more enhanced at higher pressures of 20.0 MPa than at mild pressures of 10.0 MPa at temperatures  $\cong 180^\circ\text{C}$ . In contrast, at lower temperatures ( $\cong 150^\circ\text{C}$ ) phenol production is higher at pressures of 1.0 MPa than at 20.0 MPa. This conclusion can also be extracted from Table 1, where a pressure value of 10.0 MPa was used for all the experiments using CD/DVD wastes and phenol yield was  $<1.3$  wt % in all cases, whereas for the rest of the experiments higher values were obtained.

### Effect of NaOH concentration

$\text{Na}^+ \text{OH}^-$  catalyzes the cleavage of the polymer; concentrations of  $1 \times 10^{-3}$ ,  $2 \times 10^{-3}$ , and  $5 \times 10^{-3}$  kg/L of NaOH were tested to determine the optimum quantity of NaOH. As can be observed from Figure 10a catalyst concentrations

between  $1 \times 10^{-3}$  and  $2 \times 10^{-3}$  kg/L were sufficient to foster the main reaction compared to the reaction without NaOH. Greater amounts may induce secondary reactions such as Scheme 3, producing phenol, although this effect is not sufficiently clear from Figure 10b. Furthermore, the use of higher concentrations of NaOH may also cause  $\text{Na}_2\text{CO}_3$  formation, especially in the presence of  $\text{CO}_2$ . Concentrations  $< 0.5 \times 10^{-3}$  kg/L were also tested and do not produce the desired catalytic effect; thus those experiments were not included in this work.

### Effect of solvent flow rate in mass transfer

Experiments 14 to 17 were performed to analyze the effect of solvent flow rate in mass transfer. The influence of the methanol flow rate on the yield and operational time was studied at moderately low temperatures ( $120^\circ\text{C}$ ) and pressures (10.0 MPa). As illustrated in Figures 11a–11c, the depolymerization process is enhanced using higher flow rates, although higher flow rates imply lower residence times in the reactor. These two effects were taken into account within the proposed model, and thus Figure 12 shows the variation of the effective kinetic parameter in Schemes 1 and 3. The values of  $k_{\text{eff}1}$  were found to be between 0.3 and  $8.5 \text{ min}^{-1} \text{ L}^{-1} \text{ m}^{-2}$  and for  $k_3$  were in the range between  $1.45 \times 10^{-3}$  and  $9 \times 10^{-3} \text{ min}^{-1}$

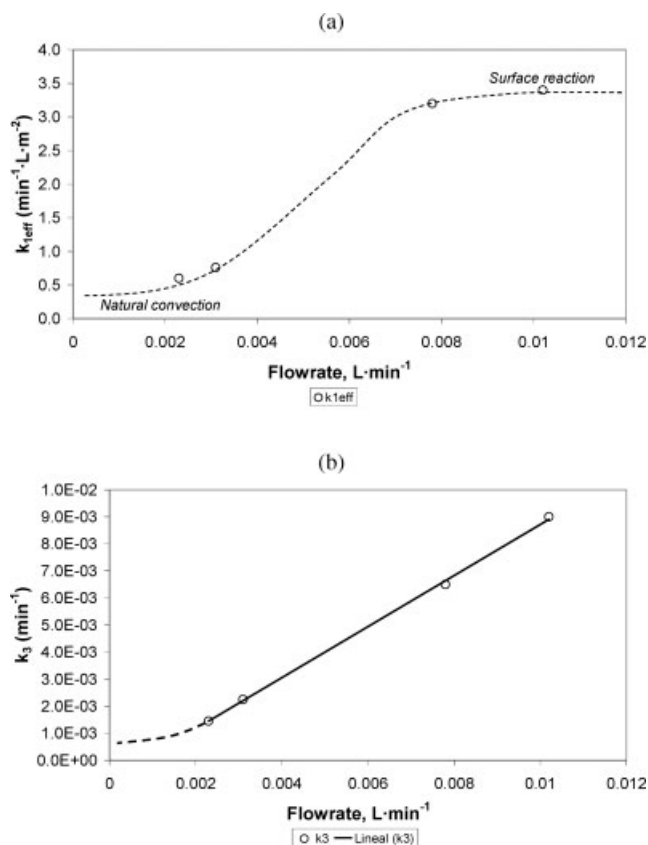


**Figure 12. Influence of mass transfer in the values of rate of reaction.**

Pressure = 10 MPa, NaOH =  $2 \times 10^{-3}$  kg/L,  $T = 120^\circ\text{C}$ .

at flow rates between  $2.3 \times 10^{-3}$  and  $10.2 \times 10^{-3} \text{ L min}^{-1}$ , respectively. As explained before the values of the effective rate of reaction are a function of both mass transfer and surface reaction. At higher flow rates mass transfer is enhanced and the effective value will be similar to the surface reaction (see Figure 12a). Similarly, at very low flow rates the reagents and products are transferred through the stagnant fluid layer surrounding the particle by a natural convection mechanism; as a result of this the value of the effective rate of reaction is much lower. For the case of concentration at the outlet of the reactor, the curve in Figure 11d shows how the concentration of BPA reaches a maximum and as the polymer disappears the concentration decreases until the reaction is completed.

### Effect of $\text{CO}_2$

In addition, a set of experiments using  $\text{CO}_2$  as cosolvent were performed aimed at softening operational conditions of the process and optimizing the process itself. Presumably, the swelling effect of  $\text{CO}_2$  on polymer materials should improve the kinetics because it increases the active surface of the solid<sup>25</sup> and also may help the mass-transport mechanism whenever the reaction system is in one homogeneous phase. Figure 13 shows the variation of cumulative mass of BPA and PhOH at different molar fractions of  $\text{CO}_2$  with time. Molar concentrations of  $\text{CO}_2$  of 9.0 and 18.3 mol % slightly enhanced the kinetics of production of BPA with respect to

results obtained for pure methanol. However, at such concentrations the production of phenol was almost doubled. Nevertheless, concentrations of 27.7 and 37.4 mol % of  $\text{CO}_2$  inhibited the reaction, obtaining about ten times less BPA product and also 50% less of phenol. To discuss this result two related causes have been found. First, the solubility of  $\text{CO}_2$  at 20.0 MPa and  $150^\circ\text{C}$  is  $x_{\text{CO}_2} = 0.423$  (predicted using the Peng–Robinson–Redlich–Kwong EoS). This means that molar fractions below this value allow for a monophasic expanded methanol, increasing the relative velocity between solvent and particles and improving mass transfer. It should be noted that NaOH will have an effect in this equilibrium probably decreasing the solubility of  $\text{CO}_2$ . In contrast, values of  $\text{CO}_2$  above this value may cause a biphasic reaction, considerably reducing the availability of methanol. Furthermore, high quantities of  $\text{CO}_2$  affect the way in which the surface of the polymer is wetted by methanol, stopping the reaction. Second,  $\text{CO}_2$  can cause the precipitation and even the carbonation of NaOH, producing  $\text{Na}_2\text{CO}_3$ . Therefore, the use of  $\text{CO}_2$  enhances BPA production, but the reduction in reaction time, <10% of total time, is not worth considering the collateral enhanced production of phenol, which will require further downstream separation, and reducing the global efficiency of the process.

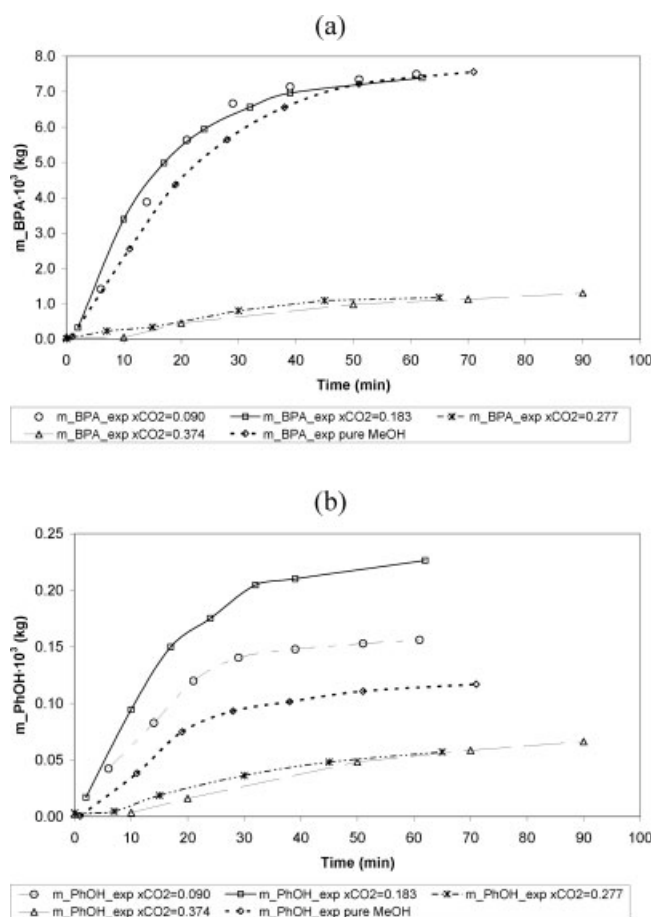


**Figure 13. Experimental cumulative mass of products at different  $\text{CO}_2$  concentrations.**

(a) Mass of BPA; (b) mass of PhOH. Pressure = 20.0 MPa, NaOH =  $2 \times 10^{-3}$  kg/L,  $T = 150^\circ\text{C}$ , MeOH flow rate =  $2.2 \times 10^{-3}$ – $5.4 \times 10^{-3} \text{ L min}^{-1}$ .



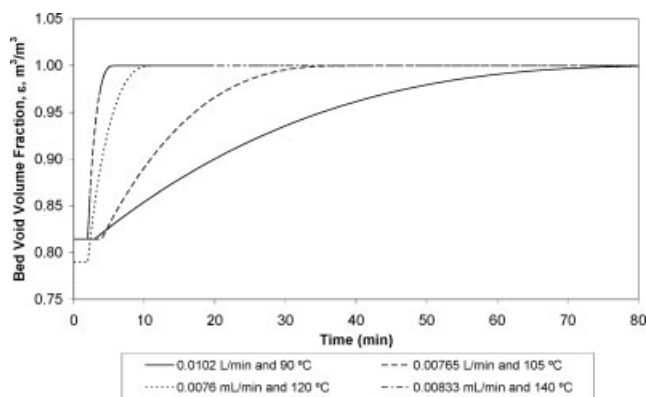


**Figure 14. Simulation of the evolution of bed void volume fraction.**

Pressure = 10.0 MPa, NaOH =  $2 \times 10^{-3}$  kg/L, flow rate =  $7.7 \times 10^{-3}$ – $10.2 \times 10^{-3}$  L min<sup>-1</sup>,  $T = 90$ – $140^\circ\text{C}$ .

### Evolution of the bed void volume fraction (BVVF)

The results of the simulation of the BVVF for experiments 10 to 13 are presented in Figure 14. At the beginning roughly 20% of the volume of the reactor is occupied by the BPA-PC particles, corresponding to a bed void volume fraction of nearly 80%. During the reaction particles react and decrease in volume, which causes an increase in the average void volume fraction of the reactor. When the reaction is completed the BVVF is one because no particles remain in the reactor, which is full of the reaction mixture (almost pure solvent).

### Modeling parameters: number of tanks in series

A number of five tanks in series was found to be the optimum value to minimize AAD% during the fitting process. This indicates that the real reactor behaves like a plug-flow reactor with a certain degree of mixing. This back-mixing is probably induced by small movements and rearrangements of the particles inside the reactor and by the proper reaction mixture (solvent) flowing up-flow.

### Conclusion

The nonstationary behavior of a depolymerization process of BPA-PC pellets in a semicontinuous tubular reactor can be accurately modeled using a simple model of  $n$  tanks in series, with  $n = 5$ . The proposed model was validated obtaining ADD% < 5–15% in all cases. The model can be used for a further scale-up of the process to pilot-plant scale. For this task, a thermodynamic model of the system must be included within the current set of model equations. Kinetics of the process have been investigated using the proposed model, determining the effect of temperature, pressure, NaOH concentration, mass transfer (solvent flow rate), and CO<sub>2</sub> addition. The production rates of BPA and DMC (main products,  $E_a = 87.6$  kJ mol<sup>-1</sup>) and phenol (main by-product,  $E_a = 34.1$  kJ mol<sup>-1</sup>) are enhanced by temperature and higher temperatures also favor the selectivity to BPA and DMC. Pressure does not significantly affect the production of BPA and DMC. Nevertheless, pressure negatively affects the production of phenol and

an optimum value of 10 MPa to minimize phenol generation was found. NaOH catalyzes the reaction from  $1 \times 10^{-3}$  kg/L; higher values are not recommended because undesired carbonylation reactions may appear. The effective rate of reaction increases with flow rate because mass transfer is enhanced. When CO<sub>2</sub> was used, biphasic behavior appeared at values of CO<sub>2</sub> > 27.7 mol % and the reaction was less selective to BPA and DMC. Because of this, the use of CO<sub>2</sub> is not recommended, although it may require additional downstream operations to recover the unreacted methanol, thus increasing energy requirements.

### Acknowledgments

This work was funded primarily by the Spanish Ministry of Education and Science, project PPQ 2003-07209 and CTQ2006-02099/PPQ. The authors would like to thank GEPESA (GE Plastics Iberica S.A) for raw polycarbonate pellets supplied. R. Piñero thanks the University of Valladolid for a PhD fellowship.

### Notation

$M_{\text{experimental}}$  = total surface area of polycarbonate particles, m<sup>2</sup>  
 $a_p$  = average surface area of a single polycarbonate particle, m<sup>2</sup>  
 $c_j$  = instant concentration of product  $j$  at the reactor outlet, mol L<sup>-1</sup>  
 $c_j^{\text{flask}}$  = concentration of product  $j$  in the flask, mol L<sup>-1</sup>  
 $c_j^{\text{in}}$  = concentration of product  $j$  at the reactor inlet, mol L<sup>-1</sup>  
 $E_a$  = activation energy, kJ mol<sup>-1</sup>  
 $F_i$  = velocity of reaction  $i$ , mol min<sup>-1</sup>  
 $k_{\text{eff1}}$  = effective rate of reaction in Scheme 1, min<sup>-1</sup> L<sup>-1</sup> m<sup>-2</sup>  
 $k_{\text{eff2}}$  = effective rate of reaction in Scheme 2, min<sup>-1</sup> L<sup>-1</sup> m<sup>-2</sup>  
 $k_3$  = rate of reaction in Scheme 3, min<sup>-1</sup>  
 $L_{\text{reactor}}$  = length of reactor vessel, m  
 $m$  = total mass of polycarbonate particles, kg  
 $m_j^{\text{flask}}$  = accumulated mass of product  $j$  in the flask, kg  
 $MW_j$  = molecular weight of component  $j$ , kg mol<sup>-1</sup>  
 $n_{\text{data}}$  = number of data considered for the fit  
 $n_j$  = number of moles of component  $j$  in the reactor, mol  
 $n_p$  = initial number of polycarbonate particles  
 $R_{\text{reactor}}$  = radius of reactor vessel, m  
 $t$  = time, min  
 $V^{\text{flask}}$  = volume recovered in the product flask, L  
 $V_{\text{reactor}}$  = total volume of reactor, L  
 $\dot{v}$  = volumetric flow rate, L min<sup>-1</sup>  
 $y_{\text{experimental}}$  = experimental data used for the fit  
 $y_{\text{calculated}}$  = simulation data produced using the model used for the fit

### Greek letters

$M_{\text{experimental}}\alpha_{ij}$  = stoichiometric coefficient of component  $j$  in the reaction  $i$   
 $\alpha_j$  = column vector of stoichiometric coefficients of component  $j$  in the different reaction schemes, that is,  $[\alpha_{1j} \alpha_{2j} \alpha_{3j}]$   
 $\varepsilon$  = bed void volume fraction,  $m_{\text{void}}^3/m_{\text{reactor}}^3$   
 $\rho_{\text{PC}}$  = density of polycarbonate particles, kg m<sup>-3</sup>

### Subscripts

$j$  = component  
 $k$  = each of the perfectly mixed tanks in series. Note that  $k$  sets of equations from Eqs. 1 to 6 are generated to solve the problem  
 $l$  = experimental data

### Literature Cited

- Allen DT, Shonnard DR. Green engineering: Environmentally conscious design of chemical processes and products. *AIChE J.* 2001; 47:1906–1910.

2. García-Serna J, Pérez-Barrigón L, Cocero MJ. New trends for design towards sustainability in chemical engineering: Green engineering. *Chem Eng J*. 2006; Submitted.
3. Benyus JM. *Biomimicry: Innovation Inspired by Nature*. New York: Harper Perennial; 1997.
4. Palmer P. *Getting to Zero Waste*. Sebastopol, CA: Purple Sky Press; 2003.
5. McDonough W, Braungart M. *Cradle to Cradle: Remaking the Way We Make Things*. New York: North Point Press; 2002.
6. Fox D, Peters EN. *Method for Recovering a Dihydric Phenol from a Scrap Polyester*. U.S. Patent Number 4 885 407; 1989.
7. Shafer SJ. *Method for Recovering Bis Hydroxy Aromatic Organic Values and Bis Aryl Carbonate Values from Scrap Aromatic Polycarbonate*. U.S. Patent Number 5 336 814; 1994.
8. Hu L-C, Oku A, Yamada E. Alkali-catalyzed methanolysis of polycarbonate. A study on recycling of bisphenol-A and dimethyl carbonate. *Polymer*. 1998;39:3841–3845.
9. Yang Y, Lu Y, Xiang H, Xu Y, Li Y. Study on methanolytic depolymerization of PET with supercritical methanol for chemical recycling. *Polym Degrad Stab*. 2002;75:185–191.
10. Goto M, Koyamoto H, Kodama A, Hirose T, Nagaoka S. Supercritical properties of fluids under high pressure. Degradation of polyethylene terephthalate in supercritical methanol. *J Phys Condens Matter*. 2002; 14:11427–11430.
11. Genta M, Iwaya T, Sasaki M, Goto M, Hirose T. Depolymerization mechanisms of poly(ethyleneterephthalate) in supercritical methanol. *Ind Eng Chem Res*. 2005;44:3894–3900.
12. Piñero R, García J, Cocero MJ. Chemical recycling of polycarbonate in a semi-continuous lab-plant. A green route with methanol and methanol–water mixtures. *Green Chem*. 2005;7:380–387.
13. Sterling WJ, McCoy BJ. Distribution kinetics of thermolytic macromolecular reactions. *AIChE J*. 2001;47:2289–2303.
14. Wan B, Kao C, Cheng W. Kinetics of depolymerization of poly(ethylene terephthalate) in a potassium hydroxide solution. *Ind Eng Chem Res*. 2001;40: 509–514.
15. Park Y, Hool JN, Curtis CW, Roberts CB. Depolymerization of styrene–butadiene copolymer in near-critical and supercritical water. *Ind Eng Chem Res*. 2001;40:756–767.
16. Kao C, Wan B, Cheng W. Kinetics of hydrolytic depolymerization of melt poly(ethylene terephthalate). *Ind Eng Chem Res*. 1998;37:1228–1234.
17. McCoy BJ, Wang M. Continuous-mixture fragmentation kinetics: Particle size reduction and molecular cracking. *Chem Eng Sci*. 1994;49:3773–3787.
18. Upendra A, Kim WB, Lee JS. Making polycarbonates without employing phosgene. *Ind Eng Chem Res*. 2004;43:1897–1914.
19. Madras G, McCoy BJ. Time evolution to similarity solutions for polymer degradation. *AIChE J*. 1998;44:647–655.
20. Madras G, McCoy BJ. Molecular-weight distribution kinetics for ultrasonic reactions of polymers. *AIChE J*. 2001;47:2341–2348.
21. Goto M, Koyamoto H, Kodama A, Hirose T, Nagaoka S, McCoy BJ. Degradation kinetics of polyethylene terephthalate in supercritical methanol. *AIChE J*. 2002;48:136–144.
22. Iwaya T, Sasaki M, Goto M. Kinetic analysis for hydrothermal depolymerization of nylon 6. *Polym Degrad Stab*. 2006;91:1989–1995.
23. Schmidt LD. *Topics in Chemical Engineering: The Engineering of Chemical Reactions*. New York: Oxford Univ. Press; 1998;9:367–393.
24. Shampine LF, Reichelt MW. The MATLAB ODE suite. *SIAM J Sci Comp*. 1997;18:1–22.
25. Bonavoglia B, Storti G, Morbidelli M. Modeling of the sorption and swelling behavior of semicrystalline polymers in supercritical CO<sub>2</sub>. *Ind Eng Chem Res*. 2006;45:1183–1200.

Manuscript received Jun. 23, 2006, and revision received Sept. 13, 2006.